Nature, source and composition of volcanic ash in sediments from a fracture zone trace of Rodriguez Triple Junction in the Central Indian Basin

M.B.L.Mascarenhas-Pereira*, B.Nagender Nath, D.V.Borole and S.M.Gupta
National Institute of Oceanography, Goa-403 004, India

Corresponding author e-mail: mariab@darya.nio.org

Abstract

Volcanic glasses associated with pumice, micro nodules and palagonite like lithic fragments were recovered from a volcanic terrain in a fracture zone defined as Rodriguez Triple Junction trace in the Central Indian Basin. Morphologically, the tephra consist predominantly of bubble wall shards with the co-occurrence of platy and blocky types. Rarity of vesicles in the shards suggests that they are formed in depths deeper than 4000 m, below the volatile fragmentation depth (VFD). Energy dispersive spectrometer (EDS) analyses have shown that the tephra have SiO_2 contents ranging from ~ 74 % - 77 % suggesting that they are mainly rhyolitic and formed from melts of siliceous composition. The depositional age of the tephra layers determined by radiolarian assemblages and excess ^{230}Th decay profile correspond to an age older than 180 kyr. The tephra are rare in sediments younger than ~ 239 ky. The beginning of the volcanic eruption contributing this volcanic ash however, cannot be estimated. Occurrence of large sized tephra suggests proximal source, probably from a local volcanic source.

Compositional and morphological contrasts, age constraints, occurrence of large sized tephra, and tectonic setting of the cored site/location suggest an intraplate volcanism, triggered by re-activation of tectonic activity in the fracture zone trace of the Indian Ocean Triple Junction during the late Pleistocene.

Introduction

Tephra layers in marine sediments provide a high-resolution and temporally precise record of volcanic activity (Paterne et al., 1988; Arculus and Bloomfield, 1992; Bednarz and Schmincke, 1994). Submarine tephra studies have become increasingly important in the course of the DSDP/ODP drilling programs, because distal tephra deposits are often the only indicators for reconstructing the petrogenetic evolution of volcanic terrains that have been eroded or buried under younger sediments (Fisher and Schmincke, 1984; Straub, 1997). The petrogenetic significance of submarine tephra layers, however, is not always easy to interpret. Marine tephra layers, mostly characterized by their glass shard fraction are known to be compositionally heterogeneous, thus enhancing the problem of compositional contrast. This may reflect pre-eruptive zoning of the magma chamber, syn- or post depositional

mixing, or mixing of material produced from different contemporaneous eruptions. Moreover, glass shard composition likely represents derivative liquids of less evolved source area magmas, the evolved composition of which obscures essential information about the magma source and their evolution (Straub, 1997).

Occurrence of glass shards in a core was observed on the flanks of a seamount, lying within the 76° 30' E fracture zone complex in the Central Indian Basin. The fracture zone was identified by Kamesh Raju et al. (1993) as a trace of the Indian Ocean Triple Junction. Earlier studies on volcanogenic sediments from other locations in the Central Indian Basin by Gupta (1988); Iyer et al. (1993, 1997); Martin-Barajas and Lallier-Vergas (1993); Pattan et al. (1999) and Sukumaran et al. (1999) have proposed insitu volcanic source, hydrothermal origin, distal fallout from Toba or Indonesian volcanic arc, respectively. Following a brief description of the geological setting of the core, we describe and discuss the morphology and chemistry of glass shards recovered from a volcanic terrain. We then discuss the relationship between the morphology and chemistry of the shards in order to decipher the origin of this volcanoclastic material.

Geological setting

The sediments used in this study were recovered using a box corer (Kastengriefer type) of dimensions 50 x 50 x 50 cm during the 61st cruise of *R.V.A.A. Sidorenko* in the year 2003. The coring was carried out at 16 °S and 75° 30' E from the flanks of a seamount in the Central Indian Basin from a water depth of 5010 m. The site is located at the southern end of 76° 30' E fracture zone (Fig 1). The core consisted predominantly of two layers (Fig 2), which were visibly distinguished as (0-6 cm) having light brown and (8-10 cm) black colors. The top layer which was ~ 6-8 cm bsf thick was identified as radiolarian ooze containing pelagic clay and the bottom layer was made up of indurated pelagic clays predominantly with volcanoclastic material. The box corer had not penetrated deeper than 20 cm due to the consolidated nature of the bottom sediment layer. The sub-sampling was carried out at 2 cm interval.

Methods

Sediments from the indurated clay section (deeper than 8 cm) were wet sieved through a 63 μm sieve with distilled water and dried at 60 °C. The fraction retained on the 63 μm sieve was split into various grain size classes and examined under a binocular microscope. Only glass shards showing no alteration (i.e. coatings of clay minerals) were separated by hand picking. Extensive Scanning Electron Microscopic (SEM) study was performed on large (> 150 μm) and small (63-150 μm) grains of ash samples to examine the morphology of the glass shards. SEM studies were carried out using a JEOL JSM-5800LV SEM at the National Institute of Oceanography, Goa, India. Operating conditions were 20 kV, 55 ŋa and were focused (3-5 μm) for accelerating voltage, probe current and beam diameter. Major oxides were analyzed using an Energy dispersive spectrometer (EDS) attachment (OXFORD Link-ISIS EDS) to the SEM. Accuracy of our analytical results is generally better than 7 % K_20 and better than 2 % for Al_20_3 and $Si0_2$. Errors in accuracy were calculated from the results obtained by us during repeated analyses of the standard and on comparison with certified values. Shards with high SiO_2 content also display high Na_2O contents (3.37 % - 6.35 %), ruling out the possibility of alkali exchange or Na volatilization under the electron beam (see Pattan et al., 1999). Morphological and chemical studies on shards represent the entire 8-20 cm.

Age was determined using Uranium-Thorium dating technique. For isotopic and biostratigraphic studies, all the 2 cm sediment section were used. For this about 2-3 mg of sediment from each section was completely dissolved by various acids (HF, HCl and $HClO_4$) in sequence in the presence of ^{232} U / ^{228} Th spike. Uranium-Thorium radiochemical separation and purification were carried out following the standard procedures of Krishnaswami and Sarin (1976). The alpha activity of the electroplated sample was assayed using ion implanted detector coupled to Octete plus Alpha spectrometer (E G & G ORTEC). In addition, biostratigraphy was determined using radiolarian assemblages for the sediment sections bearing radiolaria (following Gupta et al., 1996).

Results and Discussion

Microscopic description of the Ashes

Colorless volcanic glass shards were found dispersed through most of the core length, being abundant below 8 cm bsf. Color of the shards can be indicative of its composition (Horn et al., 1969); with colorless shards being silicic and deep brown shards of mafic composition. The sediment fraction > 63 μm consists of pumice and palagonite like lithic fragments which are highly porous with varying colors like orange, straw yellow, pale brown and off white, very few exhibit waxy luster. Next in abundance are glass shards, which in general display angular to smoothened surfaces. In addition, > 63 μm fraction also contained Fe-Mn micronodules. Micronodules appear as pitch dark black to gray color, with botryoidal structures. Only a minor fraction of the coarse fraction constituted of radiolarians (abundant above 6 cm) and other biogenic detritus.

Three different types of shards (Fig 3) can be distinguished based on their morphology 1) blocky with a few vesicles, shape of which range from spherical to oval as they form typically in hydroclastic processes; 2) platy, which are formed from the glass walls separating large flattened vesicles; and 3) bubble walled or Y-shaped, which represent the remnants of three bubble junctions, or double concave plates that formed the wall between adjoining bubbles (Fisher and Schmincke, 1984). Bubble wall shards form the dominant (70 % - 80 %) group followed by platy and blocky shards (20 % - 30 %) of the total shards. The shape of individual fragmented clast is usually related to its mode of interaction with water (Wohletz, 1983). The glass shards have concoidal to (irregular) angular fractures that likely record rapid quench fragmentation during interaction between magma and water.

Izett (1981) has shown that the shape of the shards is affected by many variables, particularly pumice shards tend to develop from relatively high viscosity rhyolitic magma with temperatures < 850 ^{o}C, whereas bubble wall shards tend to develop from lower viscosity rhyolitic magma with temperatures > 850 ^{o}C. A study by Fisher and Schminke (1984) showed that blocky shards are the result of hydroclastic fragmentation of pyroclasts contemporaneous with gas exsolution and vesiculation. There was no coverage of terrigenous or biogenic mud observed on the shards. Fractures, hydration cracks or encrustations were

not observed under SEM. All the principal shard types show textural evidence of a phreatomagmatic mode of eruption (e.g. angular, blocky with a few vesicles, non or poorly vesiculated glass fragments) (Wohletz, 1983).

Glass chemistry

We obtained EDS data on individual, fresh glass shards (Table 1). All the three morphological types were analyzed for their major constituents. These analyses were comparable to those of fresh glasses elsewhere (Fisher and Schmincke, 1984). No significant change in major oxide composition was seen as a function of glass morphology. A comprehensive table of the known volcanic fields that could have an influence on the study area is also summarized.

The glass shards can be classified as of rhyolitic in composition, using the classification of Marsh (1976), where andesites have 57 +/- 3 %, dacites have 63 +/- 3 % SiO_2 and rhyolites are more siliceous. Low TiO_2 (0.02 % - 0.13 %) is consistent with high SiO_2 concentration (74 % - 77 %) of the glass.

Age

The sediments were dated using the biostratigraphic and radiochemical methods. While the fossil zonations of radiolarian assemblages were used for biostratigraphic dating, excess ^{230}Th method ($^{230}Th_{excess}$ portion of the ^{230}Th that is not supported by the decay of ^{234}U in the sediments) was employed for radiochemical dating.

The sediments comprised of two lithic units a) a short sediment surface (~ 6 cm) of radiolarians ooze underlain by b) grayish-brown colored indurated pelagic clays section (6 - 20 cm). Only the top 6 cm section was datable biostratigraphically, since the deeper section was devoid of radiolarians. This section contained two late Quaternary radiolarian index fossils 1) *Buccinosphaera invaginata* (Haeckel) and 2) *Collosphaera tuberosa* (Haeckel). Among them, *B. invaginata* had a shorter time range and is the youngest radiolarian index fossil (Gupta et al., 1996) with the first appearance datum found at ~ 180,000 yrs (Johnson et

al., 1989). Therefore, the sediments deeper than 6 cm bsf can be identified as older than 180 kyr.

The excess ^{230}Th was calculated by subtracting the ^{234}U from the total ^{230}Th activity. The $^{230}Th_{ex}$ decay profile (Fig 4) shows fluctuations with depth probably indicating a variable input of settling fluxes of ^{230}Th with time. However, two parallel trends were seen between depths for 1) 0-6 cm and 2) 6-12 cm. The decay curve for sediment section between 0-6 cm is linear with depth and the estimated sedimentation rate was 0.32 mm/ky which corresponds to an age of ~ 175 kyr for the top 6 cm, and agrees very well with radiolarian based stratigraphy. Though, an increase in $^{230}Th_{ex}$ at 6 cm was seen, the decay profile between 6-12 cm also was linear and the sedimentation rate for the section works out to ~ 0.31 mm/ky. The base of 12 cm with this sedimentation rate would work out to ~ 370 kyr. The glasses are abundant in the sediment section deeper than 8 cm. Age at 8 cm would work out to ~ 239 kyr. Therefore, sediments younger than 239 kyr show less glass shards and show normal pelagic sediment characters. Beyond 12 cm, ^{230}Th profile is scattered and therefore not dateable. The beginning of the volcanic activity is not known as the core has not penetrated deeper. Though the basement age is ~ 50 Ma (Mukhopadhyay and Batiza, 1994), we have no evidence to determine the timing of the initiation of the activity. Whether the volcanic activity was episodic or continuous for long time cannot be deciphered with the available sediment material. The deeper sections containing broken ichthyoliths (micro fish teeth) without radiolarians may represent condensed rims of late Tertiary red pelagic clay sequence (Doyle and Riedel, 1981., Gupta, 1987, 1991).

Origin of glass shards

Many tephra beds, silicic pumice clasts and dispersed glass shards have been found in the Pliocene and Quaternary deep sea sediments of Central Indian Basin, south of the equator (Iyer and Sudhakar, 1993; Martin-Barajas and Lallier-Vergas, 1993; Pattan et al., 1999). They have been assigned to various sources like intra-basinal volcanism, distal fallout from the Youngest Toba Tuffs of Sumatra (Martin-Barajas and Lallier-Vergas, 1993; Pattan et al., 1999; see Nath, 2001 for a review), Krakatau volcano (Mudholkar and Fiji, 1995). Although Martin-Barajas and Lallier-Vergas, (1993) suggest an Indonesian arc source for C.I.B tephra and pumice, the low alkalis they report did not permit a direct Indonesian source.

Other possible sources that could have contributed to the volcanogenic material at the site are: (1) the Reunion hotspot; (2) the Kerguelen plume; (3) Broken ridge; (4) Indian Ocean Ridge volcanics; (5) Afro-Arabian flood volcanism, or (6) the Taupo volcanic center (New Zealand). All these possible sites are plotted along with our sampling location. (Fig. 5) and the composition of our shards is compared with all the above mentioned sources (Table 1). Volcanic products of the Reunion and Kerguelen hotspots tract are dominantly of effusive basaltic volcanism type (Upton and Wadsworth, 1966; Wallace, 2002; Fretzdorff and Haase, 2002). Same is the case with the volcanic products found at the Indian Ocean ridge system and at Broken ridge (Price et al., 1986; Mahoney et al., 1995), and therefore cannot be a potential source for our tephras. Though the Afro-Arabian flood volcanism and the Taupo volcanic center have a similar range of silica as in our tephras (AAS 61\8) but the depositional ages are around the time of the Oi2 cooling anomaly for Afro-Arabian volcanism at ~ 30 Ma (Ukstins Peate et al., 2003), and late Pleistocene time scale of 26.5 ka for Taupo (Sutton et al., 1995). There have been 28 intra-caldera eruption episodes from Taupo volcanic center since the 26.5 ka Oruanui caldera-forming episode and the rhyolitic eruptions of as young as 1.8 kyr are also reported (Wilson, 1993).

The ages of our core constrain a local source or sources other than Toba to have contributed these ash layers. The ages reported here for this core do not correspond to the eruptions of Toba ash. At least 3 major episodes of rhyolitic emissions have occurred in the Toba region in the past, which are identified as Oldest Toba Tuff at 840,000 +/- 30,000, Middle Toba Tuff: 500,000 +/- 5,000 and Youngest Toba Tuff at 73,000 +/- 4,000 yrs (^{40} Ar/ ^{39} Ar ages reported by Diehl et al., 1987; Chesner et al., 1991), the latter episode of YTT has been found to spread to large distances such as the northern and Central Indian Ocean (Dehn et al., 1991; Schulz et al., 1998; Pattan et al., 1999; von Rad et al., 2002).

Moreover, as against only one dominant type of shard morphology, mainly bubble wall (Rose and Chesner, 1987) found in the Toba volcanics, three types of shard morphology occur in this core, suggesting a different source, most likely from a proximal source. The glass shards of this study display a large range of SiO_2 (74 % - 77 %), K_2O (3.9 % - 6 %), Na_2O (2.36 % - 6.35 %) and low TiO_2 (0.02 % - 0.13 %). In contrast the glass shards of Toba are rhyolitic in composition with a narrow range and high contents of SiO_2 (79 % - 80 %), high K_2O (> 4.28 wt %) and low Na_2O (< 1.58 wt %) (e.g. Song et al., 2000).

Insights to the nature of major element composition was obtained from a plot of total alkalis against silica to facilitate distinction between alkaline and sub alkaline suite. The analyzed samples display a range in chemical composition of total alkalies from 7.98 % to 10.5 %. All the data point plot with in the high silica end of the rhyolitic field in the Total Alkalies vs Silica (TAS) diagram (Fig 6a). The high silica field can be subdivided into low, medium and high K groups. It is apparent that all the glasses in BC #8 core plot distinctly in the high K_2O series (Fig 6b). All the data which has been used for comparison in table 1 (other potential sources) are plotted along with our data. Expectedly, all the rhyolitic volcanics irrespective of different locations and ages (Oligocene of Afro-Arabian to Quaternary arc volcanics of Toba/IVA, and also the intraplate volcanics) fall in the high K_2O series (Fig. 6 a, b). This is important in the context of linking major element composition to known sources (in several recent papers) without considering the age. This also suggests that not all rhyolitic ashes found in the Indian Ocean can be from a single source.

Measurements of the regional distribution of maximum pyroclast size are often used to (1) estimate eruption energy, (2) determine direction to source, or (3) gain insights about the carrying capacity of the transport system (Fisher and Schmincke, 1984). The largest particle of glass shard found at BC # 8 has a diameter more than 150 μm that could even be identified under a binocular microscope. This suggests that the tephra came from a volcanically active region in the vicinity of the study area. Based on theoretical and empirical grounds, Slaughter and Hamil (1970), and Fisher (1964) predicted that the glass shards greater than 88 μm in diameter cannot be dispersed farther than 500 km from a volcanic source. The pyroclast edges are neither rounded nor abraded and thus excluding the process of reworking prior to deposition. The investigated ash therefore represents a source in the vicinity of the present study site.

The rarity of the vesicles, which is caused by high hydrostatic pressure preventing magma degassing, suggests that the glass shards are likely formed in depths deeper than 4000 m well below the Volatile fragmentation depth (Fisher and Schminke, 1984) and a critical pressure of seawater (about 3200 m water depth, Mühe et al., 1997). This is consistent with the depths noticed in our sampling location. Furthermore, our volcanic ashes of rhyolitic composition co-occur with other types of volcanogenic-hydrothermal lithic fragments. Pumice and palagonitic grains are plenty in the same sediment section. Also occur with this

volcanic suite are ferruginous sediments with nontronite and features indicative of hydrothermal nature (Mascarenhas-Pereira and Nath, MS in review). This further supports a local source. All these factors potentially rule out the possibility of Toba caldera as source, which is estimated to have expelled > 2300 Km^3 dense rock equivalent (DRE) of rhyolitic magma at ~ 74 ky dispersing its ash to distal areas in Arabian Sea, Central Indian Basin and south China Sea (Pattan et al., 1999; Schultz et al., 2002; Song et al., 2000; Dehn et al., 1991).

Having ruled out the distal sources, the tectonic setting of the study area clearly suggests a local source. The Central Indian Basin has many N-S trending fracture zones traversing it. The seamount flank where our sediments were sampled lies to the southern end of one such fracture zone. This fracture zone was identified as the trace of the Indian Ocean Triple Junction by Kamesh Raju et al., (1993). There are a number of seamounts and volcanic hills (Mukhopadhay and Batiza, 1994) lying along the fracture zones. The distribution pattern of these seamounts probably indicates that during the early history of sea-floor spreading, the upper mantle might have been trapped at different parts in the rifting oceanic crust (Sukumaran et al., 1999). Tectonic reactivation is possible for inducing hydrovolcanic activity at the seamounts, conduits and faults along these fracture zones (Iyer et. al., 1997; Mukhopadhyay et. al., 2003). One such activity must have been responsible for the deposition of the ashes studied here.

Possible mechanism of formation

Shard morphology (shape, size and vesiculation), co-occurrence with other volcanic material, age of the tephra, composition and topographic setting suggest an in-situ source owing to intraplate volcanism. Hyaloclastite deposits such as ours commonly occur around summits of seamounts near the East Pacific Rise, which are derived from hydrovolcanic activity (Smith and Batiza, 1989). Wohletz (2003) pointed out that explosive hydrovolcanism is certainly possible for depths extending to greater than 4000 m. Furthermore, the hydroclastic products (hyaloclastite) that result from magma fragmentation, associated with explosive interaction are rarely observed in deep sea cores, while they are common on seamounts (Wohletz, 2003).

Silicic magmas can contain significant portions of dissolved volatiles. During extrusion, magma volume may change significantly by crystallization and volatile exsolution. Crystallization caused by magma cooling and extrusive pressure release may promote volatile oversaturation and exsolution. Volume increases up to 50 % or more even at ambient pressures of 50 MPa (~ 5 km depth) are possible during crystallization or volatile exsolution (Burnham, 1981, 1983). This volume increase has the potential for explosive release, and it may account for extensive magma fragmentation (Dudas, 1983) such as the volcanic products associated with our study site. Magma fragmentation due to the extruding dome of viscous silicic magma may develop a carapace of hyaloclastite (Wohletz, 2003).

Conclusion

Morphological and geochemical studies carried out on volcanic glass shards recovered from a seamount environment in the Central Indian Basin have allowed us to conclude the following:

- Glass shard chemistry indicate a rhyolitic composition of the magma.
- Insitu origin (phreatomagmatic eruption) is interpreted for the volcanic ash as supported by the presence of large blocky/massive shards with a low degree of vesciculation indicating their formation by hydroclastic fragmentation.
- Since the core is located on the flanks of a seamount and in the vicinity of $76^{o}\ 30^{'}$ E fracture zone, we assume the possibility of an intraplate volcanism due to reactivation of tectonic activity in the faulted area. Comparison with geochemical data from literature on other volcanic fields in and around the central Indian basin also suggests an in-situ origin.
- Major element composition of all the siliceous tephra in the possible source areas irrespective of their ages are nearly similar and therefore caution may be exercised in using major element composition as the only criteria for determining the source of the tephras.

Acknowledgements

We thank the Director, N.I.O., for permission to communicate this manuscript. This work was carried out under the project "Environmental Impact Assessment of Polymetallic Nodule Mining" funded by the Department of Ocean Development, New Delhi. We acknowledge the help rendered by M/s Trupti, Rupali, Vinayak and Vijayan in carrying out the radiometric dating and Mr. Vijay Khedekar for his help in carrying out the SEM and EDS analysis. We are also grateful to Dr. Rahul Sharma, two anonymous reviewers and Editor Dr. Gert De Lange for their suggestions which were very useful in improving the manuscript. This is NIO's contribution

References

Arculus, R.J., Bloomfield, A.L., 1992. Major-element chemistry of ashes from sites 782, 784 and 786 in the Bonin Forearc. In: Fryer, P., Pearce, J.A., Stokking, L.B et al. (eds) Proc ODP Sci Results 125. College Station TX (Ocean Drilling Program) 125, 277-292.

Bednarz, U., Schmincke, H.-U., 1994. Composition and origin of volcaniclastic sediments in the Lau Basin (SW-Pacific), ODP Leg 135 (sites 834-893). In: Hawkins, J., Parson, L., Allan, J., et al. (eds) Proc ODP Sci Results 135. College Station TX (Ocean Drilling Program) 135, 51-74.

Burnham, C., 1983. Deep submarine pyroclastic eruptions. Econ. Geol. Monograph 5, 142-148.

Burnham, C.W., 1981. Energy of explosive volcanic eruptions. Sci. 213, 69-70.

Chesner, C.A., Rose, W.I., Deino, A., Drake, R., Westgate, J.A., 1991. Eruptive history of the Earth's largest Quaternary caldera Toba, Indonesia clarified. Geology 19, 200-203.

Dehn, J., Farrel, J.W., Schmincke, H.-U., 1991. Neogene tephrochronology from site 758 on Ninety East Ridge: Indonesian arc volcanism of the past 5 Ma. Proc. ODP, Sci. Results. 121, 273-295.

Diehl, J.F., Onstott, T.C., Chesner, C.A., Knight, M.D., 1987. No short reversals of Brunhes age recorded in the Toba Tuffs, north Sumatra, Indonesia. Geophys. Res. Lett. 14, 753 - 756.

Doyle, P.S., Riedel, W.R., 1981. Cretaceous to Neogene ichthyoliths in a giant piston core from central north Pacific. Micropaleontology 25, 4, 337-364.

Dudás, F.O., 1983. The effect of volatile content on the vesiculation of submarine basalt. Econ. Geol. Mono. 5, 134-141.

Fisher, R.V., Schmincke, H.-U., 1984. Pyroclastic rocks. Springer, Berlin Heidelberg New York.

Fisher, R.V., 1964. Maximum size, median diameter, and sorting of tephra. J. Geophys. Res. 69, 341-355.

Fretzdorff, S., Haase, K.M., 2002. Geochemistry and petrology of lavas from the submarine flanks of Réunion Island (western Indian Ocean): implication for magma genesis and the magma source. Minerology and Petrology 75, 153-184.

Gupta, S.M., 1987. Paleogene ichthyoliths from the substrates of ferromanganese encrustations and nuclei of manganese nodules from the Central Indian Basin. J. Palaeontol. Soc. India. 32, 85-91.

Gupta, S.M., 1988. Radiolarian zonation and volcanic ash layers in two Quaternary sediment cores from the Central Indian Ocean Basin. J. Palaeontol. Soc. India. 33, 59-71.

Gupta, S.M., 1991. New ichthyoliths from ferromanganese crusts and nodules from the Central Indian Ocean Basin. Micropaleontology 37, 125-147.

Gupta, S.M., Fernandes, A.A., Mohan, R., 1996. Tropical sea surface temperatures and the Earth's Eccentricity cycles. Geophysical research Letters 23, 3159-3162.

Horn. D.R., Delach, M.N., Horn, B.M., 1969. Distribution of volcanic ash layers and turbidites in the North Pacific. Geol. Soc. Am. Bull. 81, 1715-1724.

Iyer, S.D., Shyam Prasad, M., Gupta, S.M., Charan, S.N., 1997. Evidence for recent hydrothermal activity in the Central Indian Basin. Deep-Sea Res. 44, 1167-1184.

Iyer, S.D., Sudhakar, M., 1993. A new report on the occurance of zeolitites in the abyssal depth of the Central Indian Ocean Basin. Sediment. Geol. 84, 169-178.

Izett, G.A., 1981. Volcanic ash beds: recorders of Upper Cenozoic silicic pyroclastic volcanism in the western United States. J. Geophys. Res. 86, 10200-10222.

Johnson, D.A., Schneider, D.A., Nigrini, C.A., Caulet, J.P., Kent, D.V., 1989. Pliocene-Pleistocene radiolarian events and magneto-stratigraphic calibrations for the Tropical Indian Ocean. Mar. Micropaleontol. 14, 33-66.

Kamesh Raju, K.A., 1993. Magnetic lineation, fracture zones and seamounts in the Central Indian Ocean Basin. Mar. Geol. 109, 195-201.

Krishnaswami, S., Sarin, M.M., 1976. The simultaneous determination of Th, Pu, Ra isotopes, ^{210}Pb, ^{55}Fe, ^{32}Si and ^{14}C in marine suspended phases. Analytica Chimica Acta. 83, 143-156.

Le Bas, M.J., Le Maitre, R.W., Streckeisen A., Zanettin, B., 1986. A chemical classification of volcanic rocks based on the total alkali-silica diagram. J. Petrol. 27, 745-750.

Mahoney, J.J., Jones, W.B., Frey, F.A., Salters, V.J.M., Pyle, D.G., Davies, H.L., 1995. Geochemical characteristics of lavas from Broken Ridge, the Naturaliste Plateau and southernmost Kerguelen Plateau: Cretaceous plateau volcanism in the southeast Indian Ocean. Chemical Geology 120, 315-345.

Marsh, B.D., 1976. Some Aleutian andersites: their nature and source. J. Geol. 84: 27-45.

Martin-Barajas, A., Lallieri-Verges, E., 1993. Ash layers and pumice in the central Indian Basin: relationship from the formation of manganese nodules. Mar. Geol. 115, 307-329.

Mascarenhas-Pereira M.B.L., Nath B.N., 2004, in review. Geochemical signatures of hydrothermal component in the Central Indian Basin sediments recovered from a seamount flank

Mudholkar, A., Fiji, T., 1995. Fresh pumice from the central Indian Basin: a Krakatau 1883 signature. Mar. Geol. 125, 143-151.

Mühe, R., Bohrmann, H., Garbe-Schönberg, D., Kassens, H., 1997. E-MORB glasses from the Gakkel Ridge (Artic Ocean) at 87 ^{o}N: evidence for the Earth's most northerly volcanic activity. Earth and Planetary Science Letters 152, 1-9.

Mukhopadhyay, R., Batiza, R., 1994. Basinal seamounts and seamount chains of the Central Indian Ocean: probable near axis origin from a fast spreading ridge. Mar. Geophys. Res. 16, 303-314.

Mukhopadhyay, R., Iyer S.D., Ghosh A.K., 2003. The Indian Ocean Nodule Field: petrotectonic evolution and ferromanganese deposits. Earth-Science Reviews Volume 60, 1-2, 67-130.

Nath, B. N., 2001. Geochemistry of sediments. In: The Indian Ocean: A perspective. eds. by: SenGupta, R., Desa, E., Oxford & IBH; New Delhi (India) 2, 645-689.

Nath, B.N., Rao, V.P.C., Becker, K.P., 1989. Geochemical evidence of terrgenous influence in deep-sea sediments upto 8 ^{o}S in the Central Indian basin. Mar. Geol. 87, 301-313.

Paterne, M., Guichard, F., Labeyrie, J., 1988. Explosive activity of the south Italian volcanoes during the past 80,000 years as determined by marine tephrochronology. J Volcanol Geotherm Res. 34, 153-172.

Pattan, J.N., Shane, P., Banakar, V.K., 1999. New occurrence of youngest Toba Tuff in abyssal sediments of the Central Indian Basin. Mar. Geol. 155, 243-248.

Price, R.C., Kennedy, A.K., Riggs-Sneeringer, M., Frey, F.A., 1986. Geochemistry of basalts from the Indian Ocean triple junction: implications for the generation and evolution of Indian Ocean ridge basalts. Earth and Planetary Science Letters 78, 379-396.

Rickwood, P.C., 1989. Boundary lines within petrologic diagrams which use oxides of major and minor elements. Lithos 22, 247-263.

Rose, W.I., Chesner, C.A., 1987. Dispersal of ash in the great Toba eruption, 75 ka. Geology 15, 913-917.

Schulz, H., von Rad, U., Erienkeuser, H., 1998. Correlation between Arabian Sea and Greenland climate oscillations of the past 110,000 years. Nature 393, 54-57.

Slaughter, M., Hamil, M., 1970. Model for deposition of volcanic ash and resulting benthonite. Geol. Soc. Am. Bull., 81, 961-968.

Smith, T.L., Batiza, R., 1989. New field and laboratory evidence for the origin of hyaloclastite flows on seamount summits.Bull. Volcanol. 51, 96-114.

Song, S.R., Chen, C.H., Lee, M.Y., Yang, T.F., Iizuka, U., Wei, K.Y., 2000. Newly discovered eastern dispersal of the youngest Toba Tuff. Mar. Geol. 167, 303-312.

Straub, S.M., 1997. Multiple sources of Quaternary tephra layers in the Mariana Trough. J Volcanol Geotherm Res. 76, 251-276.

Sukumaran, N.P., Banerjee, R., Borole, D.V., Gupta, S.M., 1999. Some aspects of volcanic ash layers in the Cental Indian Basin. Geo-Marine Letters 18, 203-298.

Sutton, A.N., Blake, S., Wilson C.J.N., 1995. An outline geochemistry of rhyolitic eruptives from Taupo volcanic centre, New Zealand. J Volcanol Geotherm Res. 68, 153-175.

Ukstins Peate, I., Baker, J.A., Kent, A.J.R., Al-Kadasi, M., Al-Subbary, A., Ayalew, D., Menzies, M., 2003. Correlation of Indian Ocean tephra to individual Oligocene silicic eruptions from Afro-Arabian flood volcanism. Earth and Planetary Science Letters 211, 311-327.

Upton, B.G.J., Semet, M.P., Joron, J.-L., 2000. Cumulate clasts in the Bellecombe Ash Member, Piton de le Fournaise, Réunion Island, and their bearing on cumulative processes in the petrogenesis of the Réunion lavas. J Volcanol Geotherm Res. 104, 297-318.

von Rad, U., Burgath, K-P., Pervaz, M., Schulz, H., 2002. Discovery of the Toba Ash (c. 70 ka) in a high-resolution core recovering millennial monsoonal variability off Pakistan. In Clift, P.D., Kroon, D., Gaedicke, C., Craig, J., (eds). The Tectonic and Climatic Evolution of the Arabian Sea Region. Geological Society, London, Special publications. 195, 445-461.

Wallace, P.J., 2002. Volatiles in submarine basaltic glasses from the northern Kerguelen Plateau (ODP Site 1140): Implications for source region compositions, magmatic processes, and plateau subsidence. Journal of Petrology 43, 7, 1311-1326.

Wohletz, K.H., 1983. Mechanisms of hydrovolcanic pyroclast formation: Size, shape, and experimental studies. J. Volcanol. Geotherm. Res. 17, 31-63.

Wohletz, K.H., 2003. Water/magma interaction: physical considerations for the deep submarine environment. American Geophysical Union Monograph 140, 25-49.

Wilson, C.J.N., 1993. Stratigraphy, chronology, styles and dynamics of late Quaternary eruptions from Taupo volcano, New Zealand. Philosophical Transactions of the Royal Society of London. A 343, 205–306.

Figure captions

Fig 1: Tectonic features of the core location (BC #8 shown as star). Dashed lines indicate the fracture zones and the dots indicate the seamounts (from Kamesh Raju et.al., 1993). Most of the seamounts are clustered along the fracture zones. The fracture zone at 76º 30 'E represents the trace of movement of Rodriguez Triple Junction. Inset shows the different sediment types marked 1 to 5 (Nath et.al., 1989) and their description given in the legend of the figure.

Fig 2: Litholog of AAS 61/BC #8. The top 6 cm are pelagic clays with radiolarians and the 6-20 cm section is indurated clay with volcanogenic material and with some ichthyoliths.

Fig 3: Scanning electron microscope photographs of glasses investigated (scale and magnification at the bottom of the figures). a, Lithic fragment; b. to j. Glass shards are all transparent, and rhyolitic in composition. b) Shards with bubble wall, c) platy shards, probably the fragments of broken vesicles, d & h) bubble wall with 3 bubbles attached together, showing Y shaped junction, e) blocky shard with a central small vesicle, f) massive shard showing concoidal fracture, g) features indicative of hydroclastic fragmentation and typically occur due to thermal shock at magma-water interface, i) bubble wall shards with central rim intact showing normal to elongated vesicles, j) massive shard with broken vesicles, showing one elongated pipe vesicle and other broken bubble vesicle.

Fig 4: $^{230}Th_{excess}$ profile in core BC # 8 showing sedimentation rates of = 0.32mm/ky for 0-6 cm and ~ 0.31mm/ky for 6-12 cm; with an average rate of 0.41mm/ky (dotted line) for (0-12) cm.

Fig 5: Map showing the locations of known volcanic activity (described in discussion) in the Indian Ocean region with respect to our sampling location. .Symbols denote: ▲, location of present study site (AAS 61/8)., ■, Toba caldera (Westgate et al 1998)., ⬟, Toba volcanics (Ninkovitch, 1979)., ●, Reunion volcanics (Upton et al., 2000)., ▼, Afro-Arabian tephra (Ukstins et al., 2003)., ◆, Broken Ridge (ODP site 121, site 752A: Mahoney et al., 1995).,

⬣, Indian Ocean Triple junction representing Central Indian Ridge volcanics (Price et al., 1986)., ★, Kerguelen plateau (ODP site 1140: Wallace, 2002); and. arrow in the extreme right points to the Taupo volcanic site in New Zealand, which is essentially a rhyolite dominated zone.

Fig 6: (a) $Na_2O + K_2O$ vs. SiO_2 plot (TAS diagram). Nomenclature fields after Le Bas at al., (1986), with abbreviations: Tr, trachytic; T, tephrite; PhT, phonotephrite; TPh, tephri-phonolite; Ph, phonolite. The shards of AAS 61/8 plot in the rhyolitic field
(b) K_2O vs. SiO_2 plot of the shards, which shows all glasses with high SiO_2 plot in the high K series, while those of Kerguelen plateau, Broken ridge, Indian Ocean triple junction, including glass reported by Ninkovitch 1979, for the Toba caldera plot in the middle to low K series. Series boundaries after Rickwood (1989). Symbols for different volcanic field are same as in fig 5.

Table 1: Comparison of elemental data of glass shards studied here with those from other sources in the Indian Ocean area.

Sample No.	Area	SiO_2	Al_20_3	Fe_2O_3	FeO	MnO	MgO	CaO	Na_2O	K_2O	H_2O	P_2O_5	TiO_2	Na_2O+K_2O	Reference
UT1298	Toba Caldera	78.0	12.0		0.8	0.09	0.04	0.71	3.18	5.03			0.06	8.21	Westgate et al 1998
CB1	Reunion	51.0	15.0		11	0.2	3.76	7.65	4.32	1.86			3.35	6.18	Upton et al 2000
ODP 115,site 711A	Indian Ocean (Afro-Arabian)	73.0	14.0	2.42		0.18	0.28	0.47	3.92	5.23			0.53	9.15	Ukstins et al 2003
ODP 115,site 711A	Indian Ocean (Afro-Arabian)	77.0	12.0	2.27		0.11	0.13	0.21	3.54	4.77			0.38	8.31	Ukstins et al 2003
ODP 121,site 752A	Broken Ridge	49.0	14.0		11	0.18	7.66	12.2	2.1	0.18		0.13	1.6	2.28	Mahoney et al 1995
6/2	Indian Ocean triple junction	51.0	17.0		7.8	0.2	8.73	10	3.91	0.25			1.08	4.16	Price et al 1986
ODP 1140	Kerguleun	50.1	13.0	14.6		0.23	4.67	9.14	2.32	0.89	0.69	0.42	3.52	3.21	Wallace 2002
V19-151	Sunda Strait	69.6	14.2	0.7	2.2	0.12	1.4	2.5	4.7	2.3	1.5	0.12	0.49	7	Ninkovitch 1979
V19-150	Sunda Strait	69.7	13.8	0.8	1.9	0.12	1.3	1.8	4.7	2.2	2.8	0.12	0.45	6.9	Ninkovitch 1980
P915	Taupo, New Zealand	71.8	14.7	3.03		0.09	0.66	2.47	4.22	2.5			0.41	6.72	Sutton et al, 1995
Present study															
AAS 61\8	26	75.3	12.3	0.9				0.64	4.45	4.47			0.07	8.92	This study
AAS 61\8	29	75.4	12.7	0.65				0.55	5.55	3.9			0.09	9.45	This study
AAS 61\8	23	76.0	12.0	0.93				0.68	3.86	4.76			0.07	8.62	This study
AAS 61\8	2	76.3	12.2	0.91				0.66	3.37	4.61			0.05	7.98	This study
AAS 61\8	3	75.3	12.5	0.7				0.57	4.76	4.33				9.09	This study
AAS 61\8	4 (2)	76.3	11.8	0.8				0.6	3.7	4.7			0.1	8.4	This study
AAS 61\8	Grain 1	74.7	11.8	0.85		0.07		0.53	5.75	4.46			0.1	10.21	This study
AAS 61\8	Grain 2	73.9	12.4	0.72		0.09		0.62	6.35	4.17			0.04	10.52	This study
AAS 61\8	Grain 4	75.6	11.2	1.26				0.78	2.36	6			0.13	8.36	This study
AAS 61\8	Grain 5	74.8	12.1	0.9		0.05		0.74	5.01	4.52			0.07	9.53	This study
AAS 61\8	Grain 6a	75.1	11.6	0.89		0.08		0.64	4.63	5.01			0.05	9.64	This study
AAS 61\8	Grain 6b	74.8	12.0	0.81		0.07		0.55	5.57	4.6			0.07	10.17	This study
AAS 61\8	Grain 7 (2)	75.0	11.1	1.2		0.1	0.0	0.8	3.6	5.6			0.0	9.2	This study
AAS 61\8	Grain 8	74.3	12.3	0.7		0.07		0.62	6.13	4.38			0.12	10.51	This study
AAS 61\8	average	75.3	11.9	0.91		0.08	0.02	0.65	4.41	4.79			0.08	9.21	This study
AAS 61\9	min value	73.9	10.9	0.65		0.05	0.01	0.53	2.36	3.90			0.02	7.98	This study
AAS 61\10	max value	76.6	12.7	1.3		0.1	0.0	0.8	6.4	6.0			0.1	10.5	This study

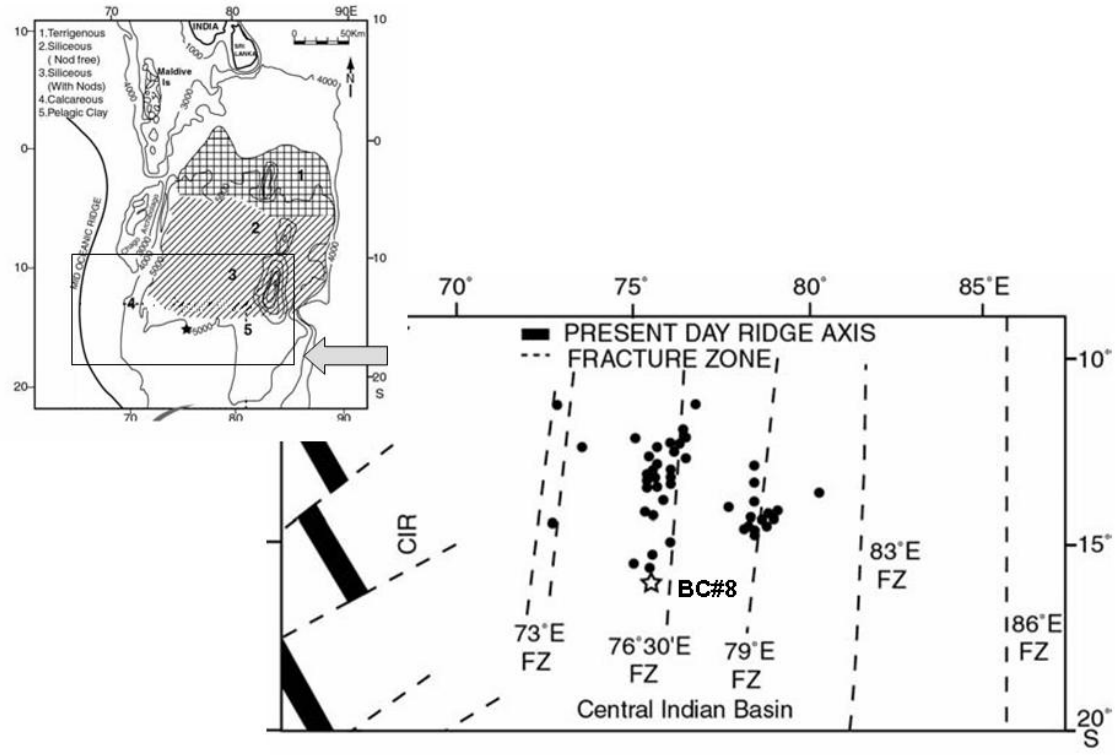

Mascarenhas-Pereira et al., (2005) Fig. 1

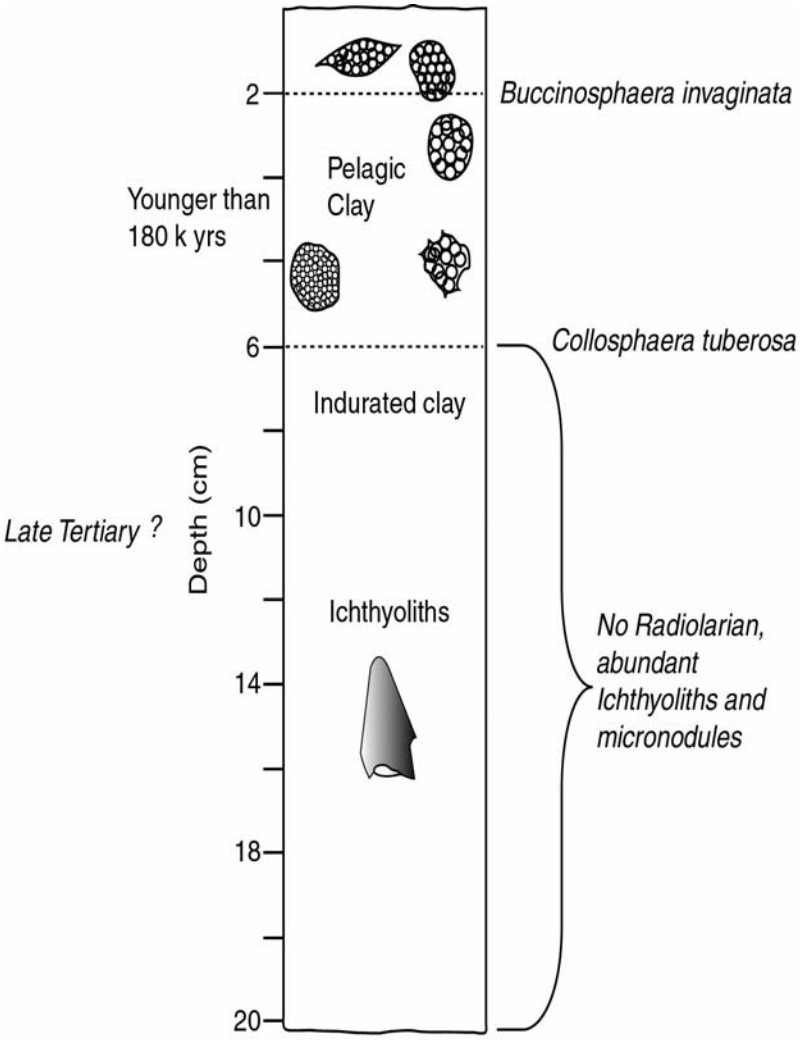

Litholog of Core AAS 61/8

Mascarenhas-Pereira et al, (2005) Fig 2.

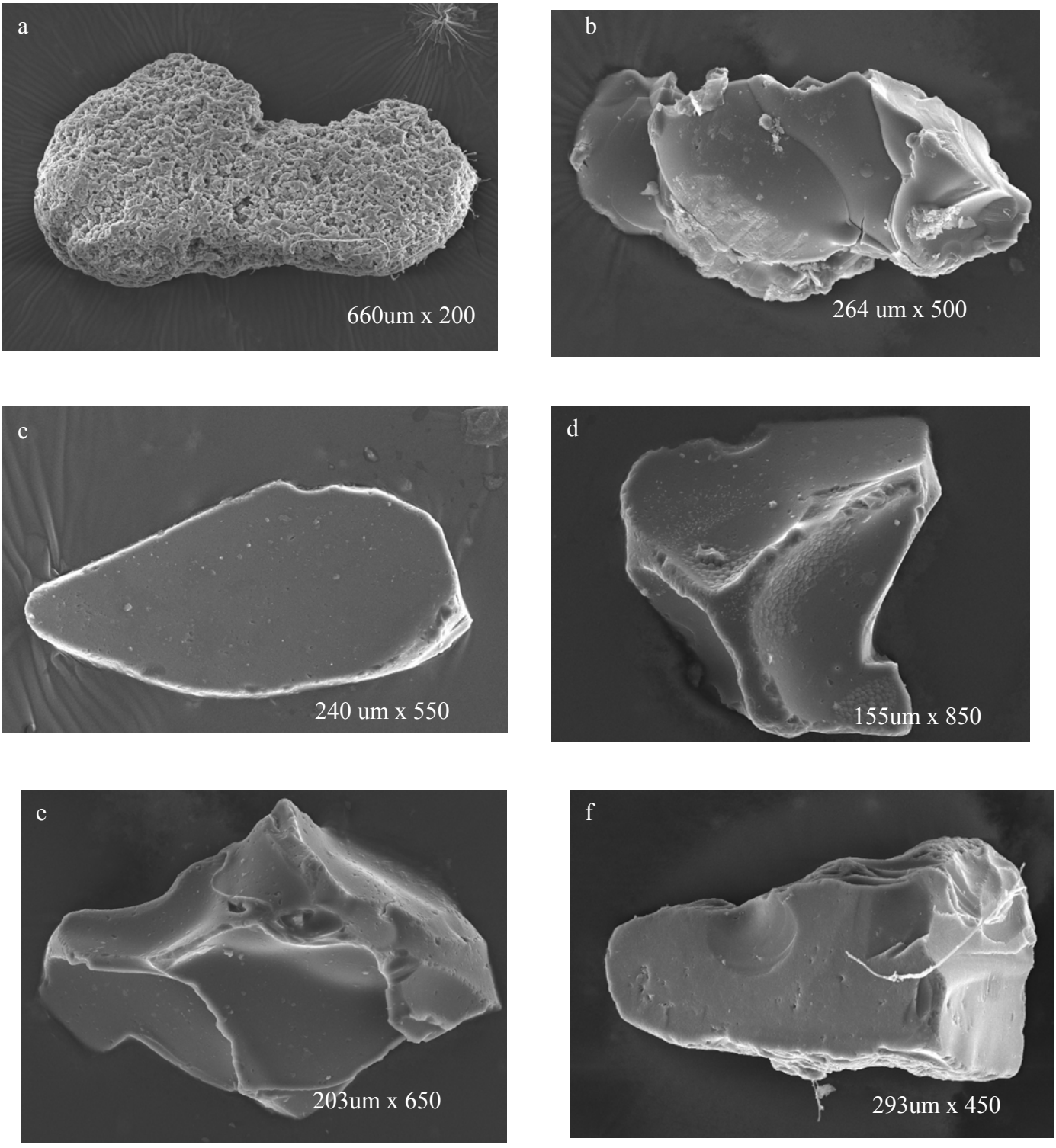

Mascarenhas-Pereira et al, (2005) Fig. 3 (a to f)

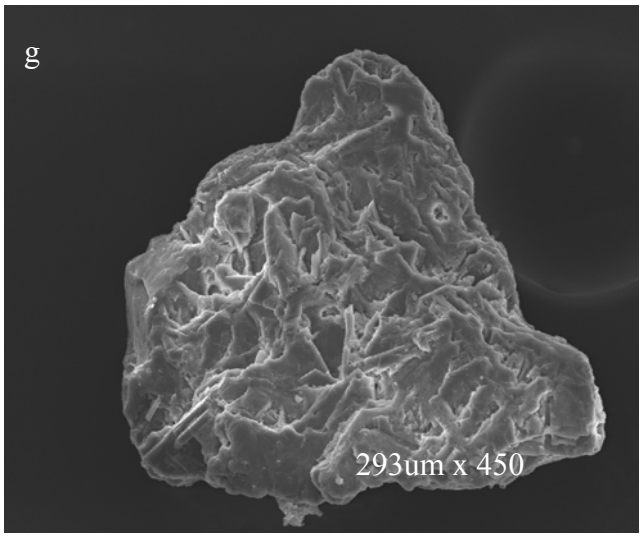

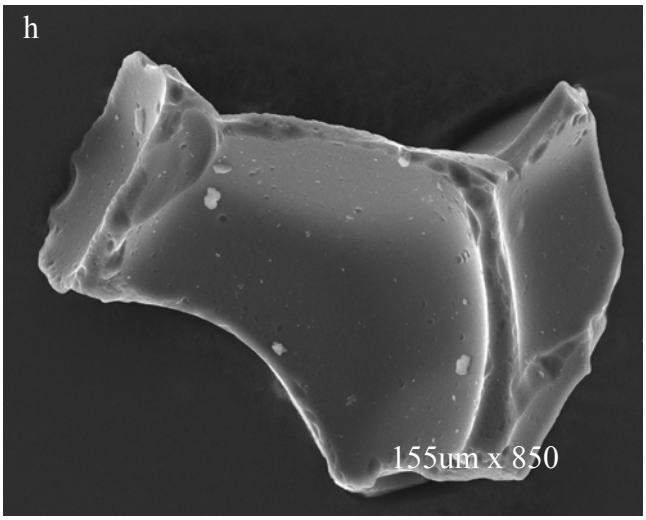

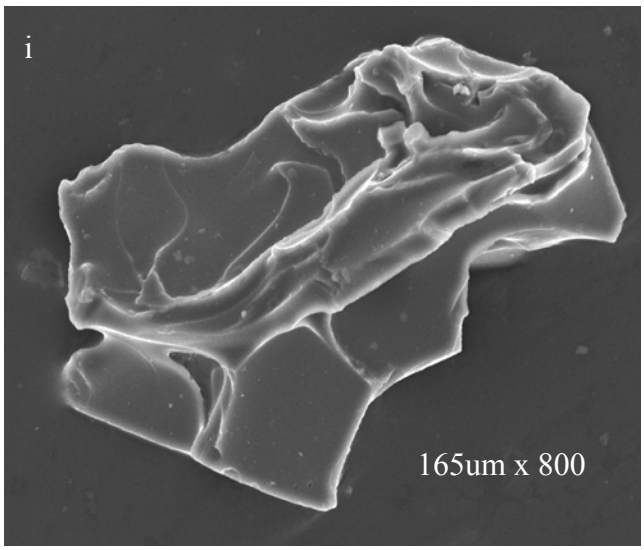

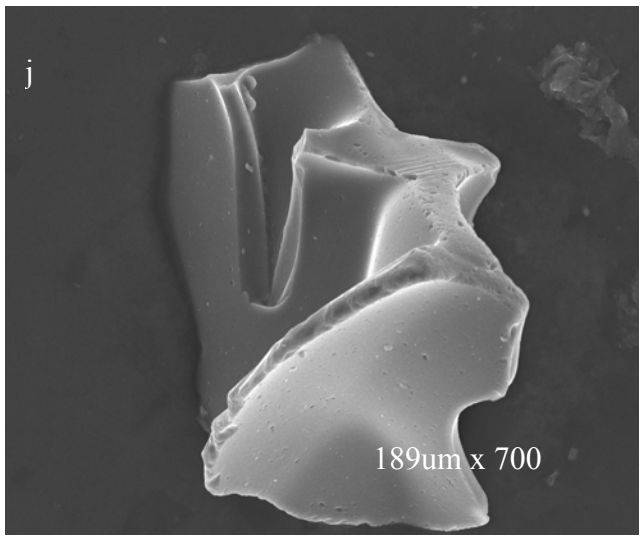

Mascarenhas-Pereira et al, (2005) Fig. 3 (g to j)

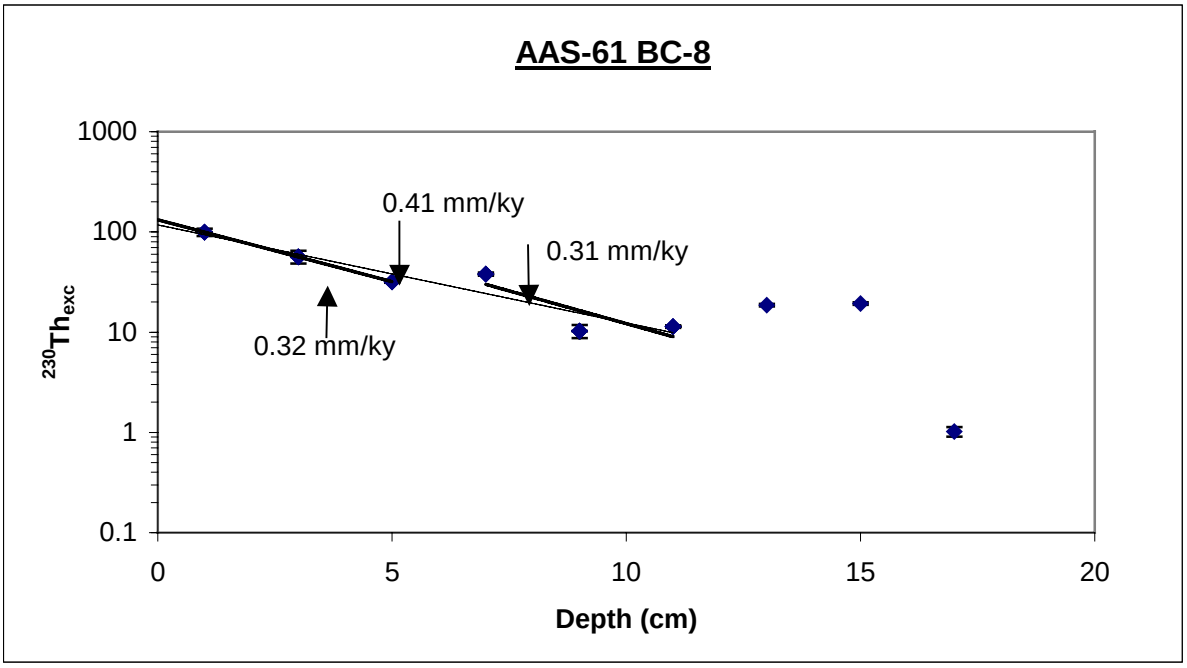

Mascarenhas-Pereira et al, (2005) Fig. 4

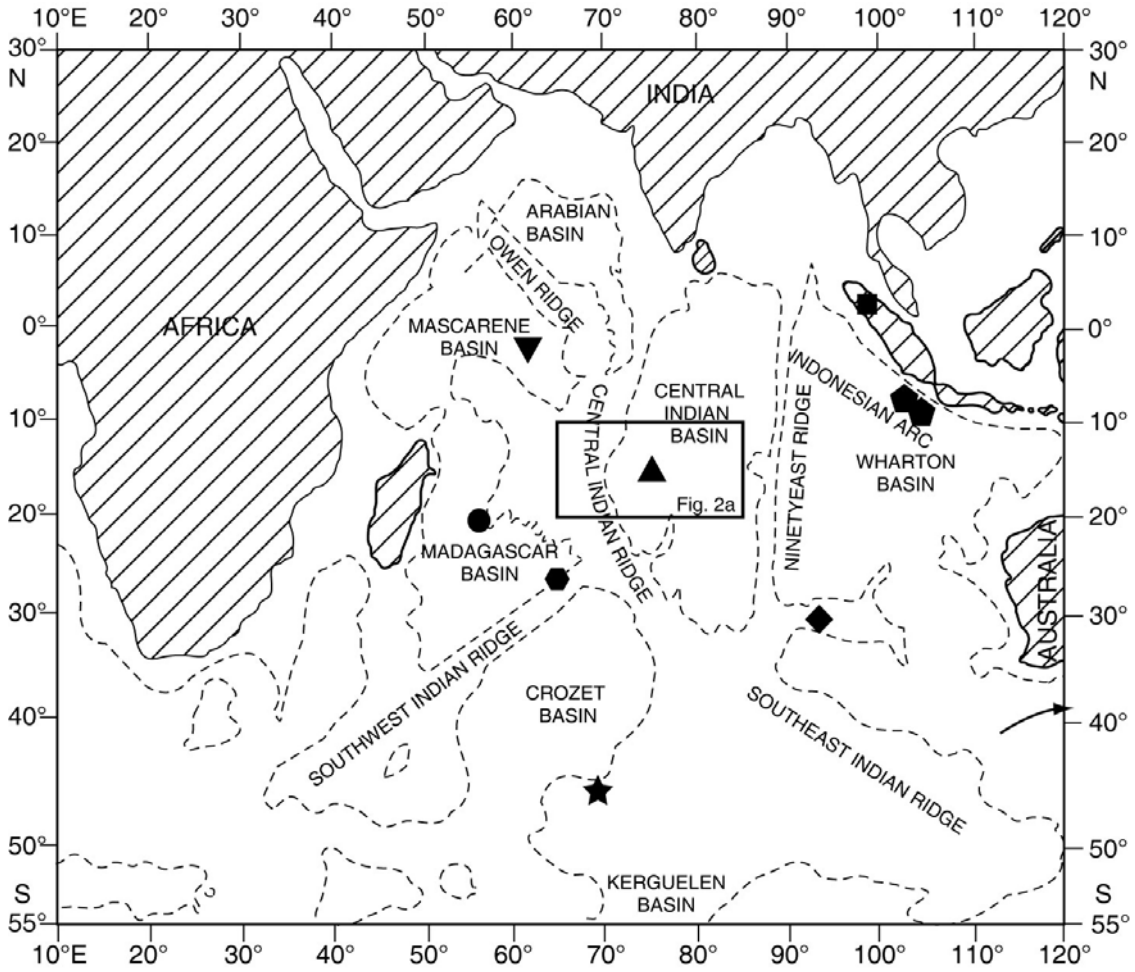

Mascarenhas-Pereira et al, (2005) Fig. 5

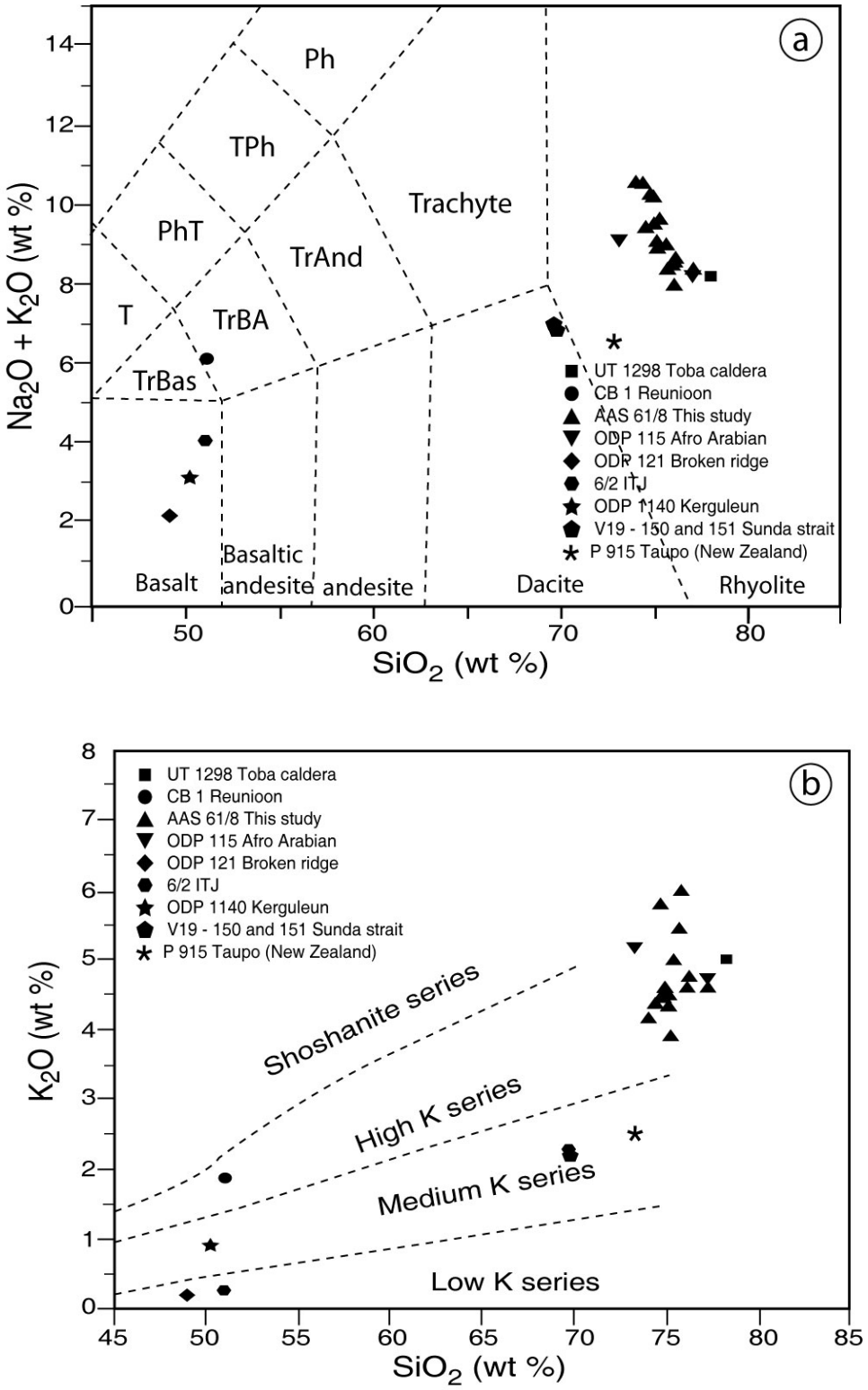

Mascarenhas-Pereira et al, (2005) Fig. 6a, b